

Workspace Modeling: Visualization and Pose Estimation of Teleoperated Construction Equipment from Point Clouds

Jingdao Chen^a, Pileun Kim^b, Dong-Ik Sun^c, Chang-Soo Han^c, Yong Han Ahn^d, Jun Ueda^e, and Yong K. Cho^{b*}

^aInstitute for Robotics and Intelligent Machines, Georgia Institute of Technology, U.S.A

^bSchool of Civil and Environmental Engineering, Georgia Institute of Technology, U.S.A

^cDepartment of Mechatronics Engineering, Hanyang University ERICA, South Korea

^dDepartment of Architectural Engineering, Hanyang University ERICA, South Korea

^eSchool of Civil and Environmental Engineering, Georgia Institute of Technology, U.S.A

E-mail: jchen490@gatech.edu, pkim45@gatech.edu, jeniussdi@naver.com, cshan@hanyang.ac.kr, yhahn@hanyang.ac.kr, jun.ueda@me.gatech.edu, yong.cho@ce.gatech.edu (*corresponding author)

Abstract –

In order to teleoperate excavators remotely, human operators need accurate information of the robot workspace to carry out manipulation tasks accurately and efficiently. Current visualization methods only allow for limited depth perception and situational awareness for the human operator, leading to high cognitive load when operating the robot in confined spaces or cluttered environments. This research proposes an advanced 3D workspace modeling method for remotely operated construction equipment where the environment is captured in real-time by laser scanning. A real-time 3D workspace state, which contains information such as the pose of end effectors, pose of salient objects, and distances between them, is used to provide feedback to the remote operator concerning the progress of manipulation tasks. The proposed method was validated at a mock urban disaster site where two excavators were teleoperated to pick up and move various debris. A 3D workspace model was constructed by laser scanning which was able to estimate the positions of the excavator and target assets within 0.1 - 0.2m accuracy.

Keywords –

Pose estimation; laser scanning; excavator

1 Introduction

Robotic agents have enormous potential to be used to perform manipulation tasks for excavation, sample collection and repair work in remote areas. In hazardous environments such as nuclear power plants or post-earthquake disaster sites, it is common for these robots to be teleoperated by human operators from a remote location [1,2]. Such challenging conditions require a high

level of situational awareness from the operator. It is difficult for human operators to efficiently and accurately carry out manipulation tasks through a teleoperation medium without clearly perceiving the pose of the robot and objects around it.

Research and field studies at major disaster relief operations such as the World Trade Center collapse showed that when mobile robots were deployed in confined spaces, the lack of perceptive data processing capability reduced the robotic skill set and added to the operator's cognitive responsibilities [2]. Armed with only a raw video feed with noisy and blurry images, operators and rescuers were unable to keep track of where the robots searched and the conditions during the deployment [2]. This problem of deficient perceptive information is amplified in the case of grasping tasks. Conventional teleoperation systems [1,3,4] make use of only a video camera that provides 2D images to the operator and the lack of depth perception makes it difficult for the operator to estimate the size and distances of unknown objects. Moreover, visual cameras do not work well at night or in adverse weather conditions. As a result, operators require a significant amount of trial and error to correctly control the robot to complete a grasping task.

An integral part of intelligent perception is transforming sensor data into knowledge and expressing that knowledge as information for use by other members in a human-robot team [5]. The idea of workspace modeling is to create a 3D representation of the robot and its surrounding environment [6–8] containing both semantic and geometric information that can be shared among all human and robotic agents in the operational team. The workspace model is constructed in real-time by processing the raw sensor data, organizing it, and labelling relevant objects [9]. Then the workspace model is used to provide visual feedback to the operator on the

task progress.

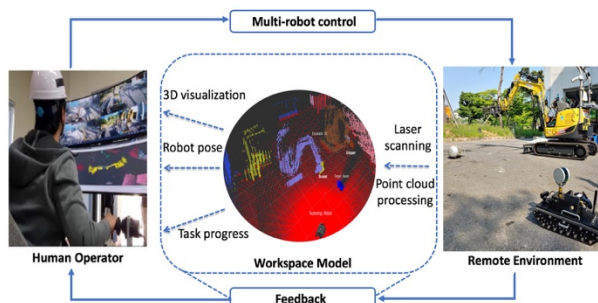


Figure 1. Feedback loop for teleoperation with 3D workspace modeling

This research proposes a context-aware 3D workspace modeling of remote equipment to improve perception and situational awareness for efficient teleoperation (Figure 1). In contrast to contemporary methods [1,4] which only provide views of the environment from the camera viewpoint to the remote operator, this research proposes a third-person viewpoint with automated state estimation and visualization of the relative pose between the end effector and salient objects. In addition, this research was validated at a large-scale outdoor environment with real construction equipment, compared to existing methods which were more focused on small to medium scale indoor environments [10,11]. To summarize, the contributions of the proposed work are as follows:

- designed a 3D workspace modeling and visualization scheme for teleoperated construction equipment
- developed an accurate algorithm for pose estimation of articulated equipment without prior dynamic models
- demonstrated the effectiveness of the 3D workspace modeling system with field trials using a multi-excavator system teleoperated in real-time

2 Literature Review

2.1 Remote Excavator System

Demand has recently been increasing for unmanned robotic excavator systems to carry out dangerous construction operations or disaster relief work. In such hazardous environments, direct human operation of excavators is unsafe due to the threat of rollover accidents, collisions, or radioactivity in the case of nuclear disaster sites. If the excavator could be robotized and teleoperated from a remote location, this would lead to a safer work environment for the human operators involved.

There are several teleoperation systems for excavators that have been studied in the literature. For example, [12] developed a excavator teleoperation system using the human arm, where sensors are attached to the operator's arm in order to detect movements so that command signals from sensors can be transmitted to the excavator. It is also possible to perform motion control with the teleoperation system by using posture sensor devices for receiving the kinematic information [13,14]. In these existing teleoperation systems, operators receive feedback either in the form of visual feedback [15,16] or force feedback [17] to monitor the interaction between the machine and the environment. More advanced excavator teleoperation systems [18,19] make use of a modular system such that a single operator can control multiple excavators with multiple end effectors at once to carry out more complex manipulation tasks. In such cases, effective feedback for teleoperation becomes even more important due to the higher risk of collision and other confounding factors such as occlusion and requirement for a larger field of view.

2.2 Workspace Visualization Systems

In a general teleoperation scenario, there are multiple ways to provide feedback to the remote operator including video feeds [3], laser scans [7], and haptic feedback [13]. In spite of these options, conventional teleoperated robots [1,4] mostly rely on a single video camera due to its simplicity and ease of use. Even when additional sensors are installed on the robot, they are poorly utilized due to the lack of information processing [2]. This causes the remote operator to have a limited field of view of surrounding objects and have limited depth perception.

There are several strategies in the literature to improve the visualization system for robot operation. [3] used a separate robot arm for visualization to overcome occlusions while performing visual servoing. However, being a primarily visual system, it still had limitations in terms of field of view and depth perception. [10] and [11] used RGBD-cameras paired with interactive visualizations to allow the operator to customize the 3D view. However, these works only considered the case of a single robot on an indoor, tabletop environment without any base displacement. [6] used 3D laser scanning to track the motion of construction equipment, but only modeled the construction equipment itself without visualizing the surrounding objects. [20] employed a multi-sensor system using four fisheye cameras and a 360° laser scanner to continuously reconstruct a 3D model of the surroundings with Simultaneous Localization and Mapping (SLAM). However, the method was only tested in static, indoor environments. Moreover, these methods have no automated object recognition or annotation of task-relevant entities,

leading to difficulty in identifying objects in cluttered or confined spaces. For the case of construction equipment, there exist algorithms for recognition [21,22] and pose estimation [23–25], but they still lack integration into a complete workspace visualization system.

3 Methodology

This research proposes a workspace modeling framework for teleoperation of remote construction equipment. As shown in Figure 1, the workspace model enables a feedback loop where the remote operator is able to simultaneously observe the effect of control inputs and interpret the remote environment from a 3D visualization interface, thus improving the situational awareness and efficiency for performing complex manipulation tasks. The workspace modeling procedure is designed to be independent from the equipment control such that the visualization and pose estimation process can remain the same regardless of any control configuration changes. The following subsections will provide details for each component of the proposed framework.

3.1 GHOST teleoperation system

This research makes use of the GHOST teleoperation system [19], which retrofits construction equipment such as excavators to be operated remotely. The manipulators are controlled wirelessly from a remote operation room equipped with monitors, joysticks and pedals. In general, each excavator can receive six different types of control signals which are assigned to the boom, arm, bucket, cabin, left track and right track respectively. Since the combination of one set of joystick and pedals is sufficient to transmit six control signals, the complete system allows a single operator to control two excavators at the same time.

However, teleoperating multiple excavators at once using conventional visualization methods is challenging even for experienced operators. Besides problems with the limited field of view and limited depth perception, the remote operator has to continuously monitor for multiple events including coordination between the excavators, occlusions, risk of collisions and risk of rollovers. This leads to a high cognitive burden for the operator, potentially causing lower efficiency and higher risk of accidents. To overcome this problem, this study implements a remote laser scanning system to provide 3D visualization of the environment surrounding the excavators, which will be described in the following sections.

3.2 Remote laser scanning system

Figure 2 shows the remote laser scanning system used to acquire a 3D reconstructed model of the excavator

workspace. The VLP-16 LiDAR was mounted on a small teleoperated tracked mobile robot and utilized to acquire real-time laser scans of the site. The VLP-16 has a range of up to 100 meters with $\pm 15^\circ$ vertical field of view. This means that the vertical angular resolution is only 2° because the VLP-16 has only 16 scan lines (channels) in the vertical direction. Thus, the scanned point cloud will be overly sparse for regions far away from the scan origin. For this reason, this study implemented an improved scanning system by installing the VLP-16 at 90° sideways and spinning it continuously with a stepper motor (refer Figure 2). In this way, the limited vertical resolution (now horizontal resolution) can be mitigated by rotating the scans horizontally, thus creating a higher resolution point cloud.

The effectiveness of 3D workspace modeling depends heavily on the point cloud update rate and resolution, which can impact the subsequent object recognition and pose estimation [26]. From the rotation mechanism discussed previously, the LiDAR scanner can generate a 360° point cloud of the surrounding environment after spinning about the vertical axis for half a revolution [27,28]. The update interval, between which the point cloud is updated to capture changes in the environment, is thus determined by the time it takes for the LiDAR scanner to spin for half a revolution. There exists a tradeoff between the rotation speed and resulting point cloud resolution due to this rotation mechanism of the laser scanner. When the rotation speed of the laser scanner is increased, the update rate increases but the point cloud resolution degrades because of the larger distance covered between consecutive scans. In contrast, when the rotation speed of the laser scanner is decreased, the point cloud resolution improves but the update rate decreases.

To find the best rotation speed, a simulation was carried out to determine the generated non-overlapping vertical scan lines when rotating the scanner. Based on this simulation, the average angle between the vertical scan lines as well as the maximum angle between the two adjacent vertical scan lines were calculated as shown in Table 1. From these results, the rotation speed corresponding to a 2.4s update interval was selected to minimize the update interval while maintaining a high horizontal resolution. This means that it is difficult for the scanner to capture rapid motions in the environment, but the higher resolution is necessary for object recognition.

Using this rotation setting, the resulting laser scanning system has a 0.25° resolution in the horizontal direction and a 0.4° resolution in the vertical direction, generating 324,000 points per update. The individual scans within each update are registered by multiplying by a rotation matrix, calculated from the rotation angle of the stepper motor. The laser scan data is published

wirelessly to the operation room as a ROS (Robot Operating System) message.

Table 1. Relationship between update interval and horizontal angular resolution

Update Interval	1.2s	1.4s	2.1s	2.4s	2.5s	2.9s
# vertical lines	374	447	641	720	523	927
avg. horiz. resolution (°)	0.48	0.40	0.28	0.25	0.34	0.19
max. horiz. resolution (°)	0.50	0.43	0.29	0.25	0.40	0.28

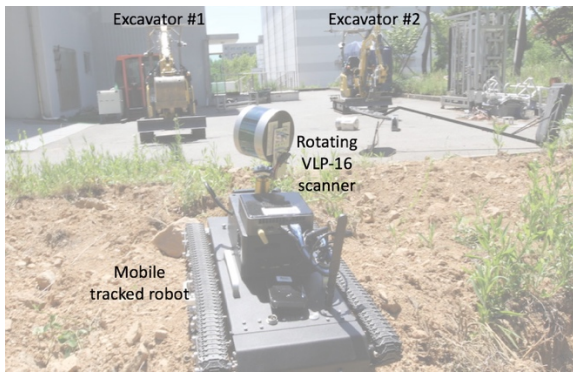


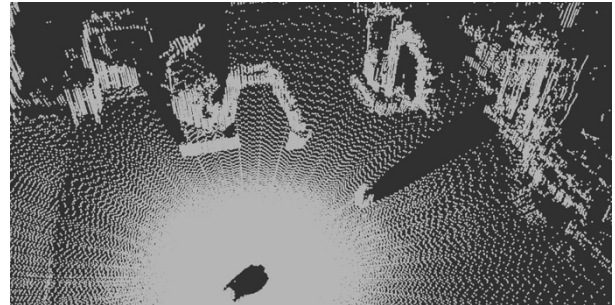
Figure 2. Remote laser scanning system

3.3 Point cloud pre-processing and segmentation

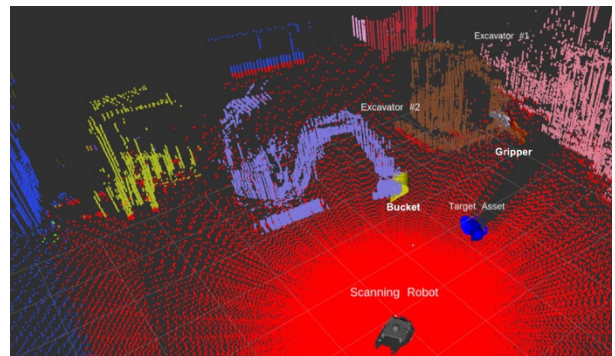
Processing the point clouds in real-time is challenging due to noisy sensor data, limited resolution of the laser scanner (refer Section 3.2), limited data bandwidth, and motion blurring of objects. Moreover, the point cloud is dynamically changing due to the movement of equipment and in the scene, meaning that it has to be processed incrementally.

A voxel grid filter is first used to equalize the point cloud resolution to 0.1m throughout the scene. This serves a dual purpose of allowing more consistent segmentation as well as speeding up the processing time by downsampling the point cloud. Next, the point cloud scene is segmented into smaller units corresponding to individual objects to enhance visualization of the scene. To meet the real-time constraint, the fast segmentation method of [29] is used. The ground plane is first segmented using the RANSAC algorithm [30] to estimate the 3D plane parameters. Alternatively, for the case of non-flat ground, the ground segmentation algorithm from [21] can be used. From the remaining points, Euclidean clustering is used to form clusters

consisting of points that neighbor each other within a margin of 0.15m. As new scan points are acquired, they are matched to the closest existing clusters and each cluster is then updated. New scan points also cause new clusters to be initiated if no neighboring clusters are found. This allows the segmentation process to occur incrementally, similar to the method used in [31].



(a) Raw point cloud acquired by laser scanning



(b) Segmented point cloud showing relevant entities

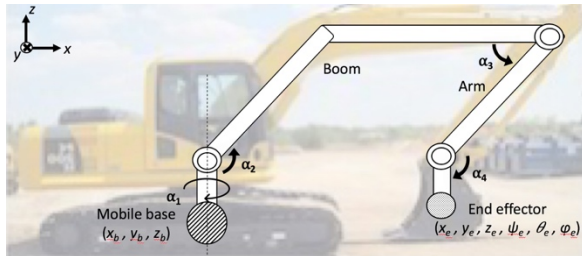
Figure 3. Point cloud segmentation results for a scene with two excavators and a single target asset

Next, the following relevant entities are automatically labeled in the scene: (i) laser-scanning robot, (ii) construction equipment, and (iii) target assets for manipulation tasks. The position of the laser-scanning robot can be easily determined as the origin of the point cloud scan. On the other hand, the positions of various construction equipment can be determined by using the method in [21], where a feature descriptor is computed for each point cloud cluster and classified with a pre-trained classifier. Finally, the point cloud clusters for objects lying on the ground close to the construction equipment are labelled as potential targets for manipulation.

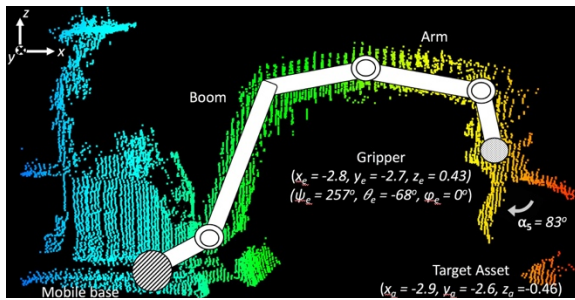
Figure 3 shows an example of the segmentation results for a scene with two excavators and a single target asset. The segmentation results are additionally overlaid with CAD models of the end effectors (bucket or gripper) and other relevant entities (e.g. target asset and scanning robot) to enhance the visualization. From Figure 3, the

raw point cloud data is extremely blurry, and it is difficult to keep track of the movement of objects in the robot workspace. However, with automated segmentation and annotation of the point cloud data, the remote operator is able to better perceive the robot workspace.

3.4 Point cloud-based pose estimation



(a) Model parameters for excavator joint configuration



(b) Pose estimation result for a gripper and a target asset

Figure 4. Excavator pose estimation

Figure 4a shows the model of the excavator joint configuration used in this study. For each excavator, the robot pose can be described in terms of the following variables: (x_b, y_b, z_b) , position of the mobile base; α_1 , rotation of the mobile base with respect to the z -axis; α_2 , rotation of the boom relative to the mobile base; α_3 , rotation of the arm relative to the boom; α_4 , rotation of the end effector relative to the arm. Similarly, the pose of the end effector can be described in terms of the following variables: (x_e, y_e, z_e) , the position of the end effector and $(\psi_e, \theta_e, \phi_e)$, yaw, pitch, roll angles of the end effector with respect to the world frame. In addition, the variable α_5 is used to describe the opening angle of the end effector if a gripper is used.

To perform pose estimation on articulated equipment such as excavators, the strategy used is to approximate each joint as a line segment and use line detection algorithms to extract corresponding segments from the point cloud. Due to the noisy nature of the point cloud, robust parameter estimation methods such as RANSAC [30] and PCA [32] are used. Then the tangent direction of each line segment

is used to estimate the joint rotation angles α . Empirically, using RANSAC for detecting the boom and PCA for detecting the arm gives the best results. Next, the end effector points are segmented by taking the rightmost points of the excavator after correcting for rotation. (x_e, y_e, z_e) is calculated by taking the centroid of this segment whereas $(\psi_e, \theta_e, \phi_e)$ can be inferred from the internal joint angles. The gripper opening angle, α_5 , is estimated by taking the width of the end effector segment after correcting for rotation. On the other hand, to perform pose estimation of a target asset for manipulation, the position, (x_a, y_a, z_a) , is first estimated by taking the centroid of the corresponding point cloud segment. Then the orientation, α_a is estimated by extracting the convex hull and solving for the minimum bounding box [33]. Each step of the pose estimation process also employs error correction using the smooth motion constraint. That is, if a new prediction differs from the previous prediction by more than a predetermined threshold (e.g. due to outlier data), the new prediction is discarded.

Figure 4b shows an example of the point-cloud based pose estimation result for an excavator equipped with a gripper. The segmentation can be computed in 0.05 - 0.1s whereas the pose estimation can be computed in 0.02 - 0.03s. The delay in showing the 3D visualization depends on network latency, but is usually within 1s. The final 3D workspace model is displayed through an interactive user interface. The remote operator is allowed to select the target asset of interest for manipulation. The user interface will then display task progress in terms of grasping the target asset.

4 Results

4.1 Experimental setup

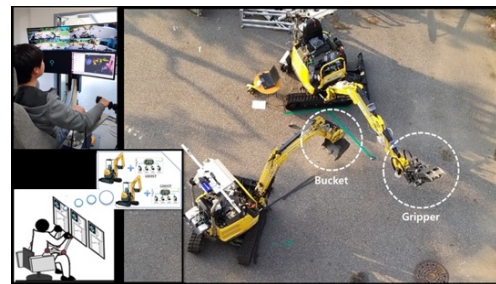


Figure 5. Experimental setup of two excavators at a mock urban disaster site.

The experimental setup consists of two robotic unmanned excavators deployed at a mock urban disaster site (Figure 5). The operator has two options to remotely

monitor the test environment: (i) 2D images from cameras mounted on the excavator roof and (ii) 3D visualization obtained from the mobile laser scanning system. One excavator is equipped with a gripper as the end effector whereas the other excavator is equipped with a bucket. Using one or both of the excavators, the operator is tasked with carrying out various manipulation tasks such as picking up miscellaneous wreckage and moving them to a specified location. The accuracy and effectiveness of the proposed workspace modeling and visualization system is then validated using the pose estimation accuracy.

4.2 Pose estimation accuracy

The pose estimation results are visualized as shown in Figure 6. Note that this evaluation only considers a single excavator, but the proposed system is able to estimate the poses of multiple excavators simultaneously. The left 4 columns show results for a propane tank as the target object whereas the rightmost column show results for a plastic container as the target object. From the 2D images of the operator view, it is difficult to perceive whether the gripper is in line with the target object and the distance of the gripper to the target object. On the other hand, the 3D visualization provides helpful information in terms of physical distances and poses that can assist the remote operator in decision making.

As shown in Table 2, the pose estimation accuracy is measured using three metrics: (i) error in estimating the distance from the center of the end effector to the center of the target asset, d_1 , (ii) error in estimating the distance from the center of the end effector to the ground, d_2 , (iii) error in estimating the distance from the center of the end effector to the center of the excavator body, d_3 . The

accuracy of the proposed method is compared against two baselines methods: (i) simple line-fitting with linear least-squares regression [34] and (ii) Iterative Closest Point (ICP) [35] to fit the end effector model to the scanned point cloud. Results show that the proposed method achieved lower pose estimation errors compared to the two baseline methods. This is because the scanned point cloud is too noisy and has low resolution for simple line-fitting or ICP to work, whereas the proposed method is able to estimate the pose parameters from point clouds more robustly.

Table 2. End effector pose estimation error

Method	d_1 error (m)	d_2 error (m)	d_3 error (m)
Simple line-fitting [34]	0.93±1.06	0.39±0.50	0.15±0.07
ICP [35]	0.15±0.11	0.10±0.07	0.24±0.26
Our method	0.13±0.07	0.09±0.09	0.10±0.08

5 Conclusions

In summary, this research proposed a workspace modeling system for teleoperated construction equipment based on laser scanning. Through field tests at a mock urban disaster site, the constructed 3D workspace model was demonstrated to be able to estimate the positions of the excavator and target assets accurately and improve the performance of human operators on manipulation tasks. This represents an important step towards achieving the goal of improving the efficacy of remote robot operation, reducing human operator needs, and reducing the operator's cognitive burden during teleoperation. For future work, the method will be extended to more types of heavy equipment such as

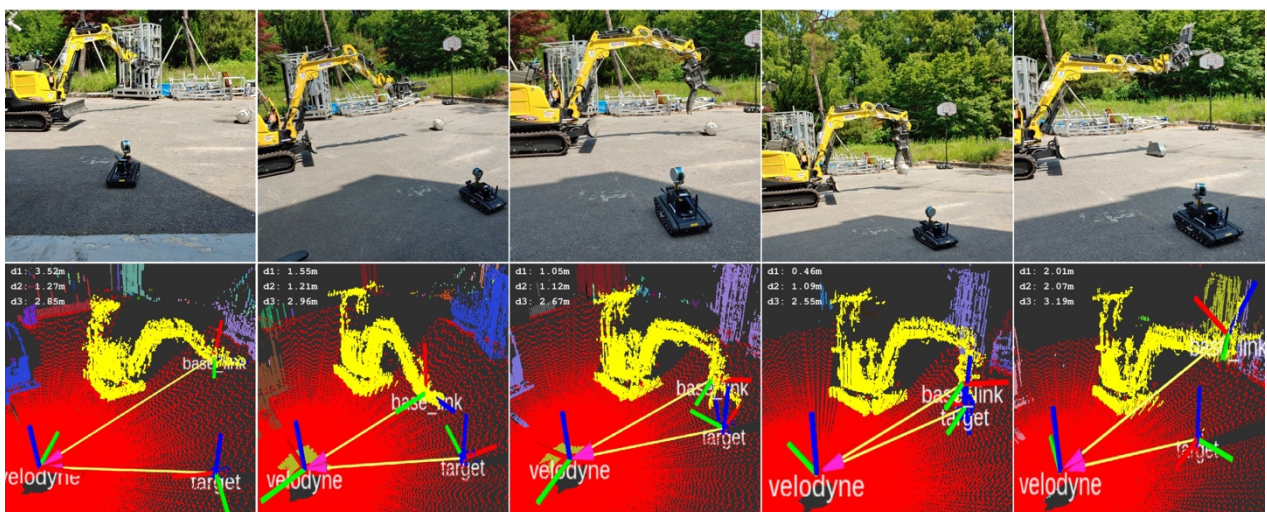


Figure 6: Visualization and pose estimation of excavator workspace. The top row shows 2D images of the scene whereas the bottom row shows the corresponding 3D visualization

loaders and dump trucks and further evaluated in more challenging manipulation scenarios.

Acknowledgements

This material is based upon work supported by the Air Force Office of Scientific Research (Award No. FA2386-17-1-4655) and by the Technology Innovation Program (No. 2017-10069072) funded by the Ministry of Trade, Industry & Energy (MOTIE, Korea). Any opinions, findings, and conclusions or recommendations expressed in this material are those of the authors and do not necessarily reflect the views of the United States Air Force or MOTIE.

References

- [1] T. Sakaue, S. Yoshino, K. Nishizawa, K. Takeda, Survey in Fukushima Daiichi NPS by Combination of Human and Remotely-Controlled Robot, in: IEEE International Symposium on Safety, Security and Rescue Robotics (SSRR), 2017.
- [2] J. Casper, R.R. Murphy, Human – Robot Interactions During the Robot-Assisted Urban Search and Rescue Response at the World Trade Center, IEEE Transactions on Systems, Man and Cybernetics. 33 (2003) 367–385. doi:10.1109/TSMCB.2003.811794.
- [3] D. Nicolis, M. Palumbo, A.M. Zanchettin, P. Rocco, Occlusion-Free Visual Servoing for the Shared Autonomy Teleoperation of Dual-Arm Robots, IEEE Robotics and Automation Letters. 3 (2018) 796–803. doi:10.1109/LRA.2018.2792143.
- [4] G. Beraldo, M. Antonello, A. Cimolato, E. Menegatti, L. Tonin, Brain-Computer Interface Meets ROS: A Robotic Approach to Mentally Drive Telepresence Robots, in: 2018 IEEE International Conference on Robotics and Automation (ICRA), 2018: pages 1–6. doi:10.1109/ICRA.2018.8460578.
- [5] R.R. Murphy, Human-robot interaction in rescue robotics, IEEE Transactions on Systems, Man, and Cybernetics, Part C (Applications and Reviews). 34 (2004) 138–153. doi:10.1109/TSMCC.2004.826267.
- [6] C. Wang, Y.K. Cho, Smart scanning and near real-time 3D surface modeling of dynamic construction equipment from a point cloud, Automation in Construction. 49 (2015) 239–249. doi:10.1016/j.autcon.2014.06.003.
- [7] Y.K. Cho, C. Wang, P. Tang, C.T. Haas, Target-Focused Local Workspace Modeling for Construction Automation Applications, Journal of Computing in Civil Engineering. 26 (2012) 661–670.
- [8] J. Chen, Y. Fang, Y.K. Cho, Real-Time 3D Crane Workspace Update Using a Hybrid Visualization Approach, Journal of Computing in Civil Engineering. 5 (2017). doi:10.1061/(ASCE)CP.1943-5487.0000698.
- [9] J. Chen, Y.K. Cho, J. Ueda, Sampled-Point Network for Classification of Deformed Building Element Point Clouds, in: Proceedings of the 2018 IEEE Conference on Robotics and Automation (ICRA), 2018.
- [10] T. Zhang, Z. McCarthy, O. Jow, D. Lee, X. Chen, K. Goldberg, P. Abbeel, Deep Imitation Learning for Complex Manipulation Tasks from Virtual Reality Teleoperation, in: 2018 IEEE International Conference on Robotics and Automation (ICRA), 2018: pages 1–8. doi:10.1109/ICRA.2018.8461249.
- [11] D. Kent, C. Saldanha, S. Chernova, A Comparison of Remote Robot Teleoperation Interfaces for General Object Manipulation, in: ACM/IEEE International Conference on Human-Robot Interaction (HRI), 2017: pages 1–8. <http://www.rail.gatech.edu/wp-content/uploads/2017/06/hri2017-kent-saldanha-chernova.pdf>.
- [12] D. Kim, J. Kim, K. Lee, C. Park, J. Song, D. Kang, Excavator tele-operation system using a human arm, Automation in Construction. 18 (2009) 173–182. doi:https://doi.org/10.1016/j.autcon.2008.07.002.
- [13] T. Hirabayashi, J. Akizono, T. Yamamoto, H. Sakai, H. Yano, Teleoperation of construction machines with haptic information for underwater applications, Automation in Construction. 15 (2006) 563–570. doi:https://doi.org/10.1016/j.autcon.2005.07.008.
- [14] Soon-Young Yang, Sung-Min Jin, Soon-Kwang Kwon, Remote control system of industrial field robot, in: 2008 6th IEEE International Conference on Industrial Informatics, 2008: pages 442–447. doi:10.1109/INDIN.2008.4618140.
- [15] K. Yoshihiro, A remotely controlled robot operates construction machines, Industrial Robot: An International Journal. 30 (2003) 422–425. doi:10.1108/01439910310492185.
- [16] T. Sasaki, K. Kawashima, Remote control of backhoe at construction site with a pneumatic robot system, Automation in Construction. 17 (2008) 907–914. doi:https://doi.org/10.1016/j.autcon.2008.02.004.
- [17] J. Hou, D. Zhao, A new force feedback algorithm for hydraulic teleoperation robot, in: 2010

- International Conference on Computer Application and System Modeling (ICCASM 2010), 2010: pages V15-15-V15-18. doi:10.1109/ICCASM.2010.5622490.
- [18] E. Rohmer, K. Yoshida, E. Nakano, A Novel Distributed Telerobotic System for Construction Machines Based on Modules Synchronization, in: 2006 IEEE/RSJ International Conference on Intelligent Robots and Systems, 2006: pages 4199–4204. doi:10.1109/IROS.2006.281913.
- [19] D. Sun, S. Lee, Y. Lee, S. Kim, J. Ueda, Y.K. Cho, Y. Ahn, C. Han, Assessments of Intuition and Efficiency: Remote Control of the End Point of Excavator in Operational Space by Using One Wrist, ASCE International Conference on Computing in Civil Engineering 2019. (2019) 273–280. doi:10.1061/9780784482438.035.
- [20] S.-H. Kim, C. Jung, J. Park, Three-Dimensional Visualization System with Spatial Information for Navigation of Tele-Operated Robots, Sensors. 19 (2019). doi:10.3390/s19030746.
- [21] J. Chen, Y. Fang, Y.K. Cho, C. Kim, Principal Axes Descriptor for Automated Construction-Equipment Classification from Point Clouds, Journal of Computing in Civil Engineering. (2016) 1–12. doi:10.1061/(ASCE)CP.1943-5487.0000628.
- [22] J. Chen, Y. Fang, Y.K. Cho, Performance evaluation of 3D descriptors for object recognition in construction applications, Automation in Construction. 86 (2018) 44–52. doi:10.1016/j.autcon.2017.10.033.
- [23] C.-J. Liang, K.M. Lundeen, W. McGee, C.C. Menassa, S. Lee, V.R. Kamat, Fast Dataset Collection Approach for Articulated Equipment Pose Estimation, in: Computing in Civil Engineering 2019, n.d.: pages 146–152. doi:10.1061/9780784482438.019.
- [24] C. Chen, Z. Zhu, A. Hammad, W. Ahmed, Vision-Based Excavator Activity Recognition and Productivity Analysis in Construction, in: Computing in Civil Engineering 2019, n.d.: pages 241–248. doi:10.1061/9780784482438.031.
- [25] J. Kim, S. Chi, M. Choi, Sequential Pattern Learning of Visual Features and Operation Cycles for Vision-Based Action Recognition of Earthmoving Excavators, in: Computing in Civil Engineering 2019, n.d.: pages 298–304. doi:10.1061/9780784482438.038.
- [26] J. Park, P. Kim, Y.K. Cho, J. Kang, Framework for automated registration of UAV and UGV point clouds using local features in images, Automation in Construction. 98 (2019) 175–182. doi:https://doi.org/10.1016/j.autcon.2018.11.024.
- [27] P. Kim, J. Chen, Y.K. Cho, Automated Point Cloud Registration Using Visual and Planar Features for Construction Environments, ASCE Journal of Computing in Civil Engineering. 32 (2018) 1–13. doi:10.1061/(ASCE)CP.1943-5487.0000720.
- [28] P. Kim, Y.K. Cho, J. Chen, Target-Free Automatic Registration of Point Clouds, ISARC. Proceedings of the International Symposium on Automation and Robotics in Construction. 33 (2016) 1–7.
- [29] M. Himmelsbach, F. v. Hundelshausen, H.-. Wuensche, Fast segmentation of 3D point clouds for ground vehicles, in: 2010 IEEE Intelligent Vehicles Symposium, 2010: pages 560–565. doi:10.1109/IVS.2010.5548059.
- [30] M. a Fischler, R.C. Bolles, Random Sample Consensus: A Paradigm for Model Fitting with Applications to Image Analysis and Automated Cartography, Communications of the ACM. 24 (1981) 381–395. doi:10.1145/358669.358692.
- [31] R. Dubé, M.G. Gollub, H. Sommer, I. Gilitschenski, R. Siegwart, C. Cadena, J. Nieto, Incremental-Segment-Based Localization in 3-D Point Clouds, IEEE Robotics and Automation Letters. 3 (2018) 1832–1839. doi:10.1109/LRA.2018.2803213.
- [32] R.B. Rusu, Semantic 3D Object Maps for Everyday Manipulation in Human Living Environments, KI - Künstliche Intelligenz. 24 (2010) 345–348.
- [33] J. O'Rourke, Finding minimal enclosing boxes, International Journal of Computer & Information Sciences. 14 (1985) 183–199. doi:10.1007/BF00991005.
- [34] I.-K. Lee, Curve reconstruction from unorganized points, Computer Aided Geometric Design. 17 (2000) 161–177. doi:https://doi.org/10.1016/S0167-8396(99)00044-8.
- [35] S. Kwon, M. Lee, M. Lee, S. Lee, J. Lee, Development of optimized point cloud merging algorithms for accurate processing to create earthwork site models, Automation in Construction. 35 (2013) 618–624. doi:https://doi.org/10.1016/j.autcon.2013.01.004.